

0.223, the latter a N galaxy having $z = 0.306$. We measured the profile at 7 equidistant wavelength positions symmetric around the expected line centre. We show in Fig. 4 the profile of the $P\alpha$ line of the quasar; an estimated error bar is indicated. The accuracy of the profile compares favourably with $P\alpha$ profiles obtained for some other objects by two American groups (Puetter et al., 1981, *Astrophys. J.*, **243**, 345; Soifer et al., 1981, *Astrophys. J.*, **243**, 369). During the same run we obtained Balmer line profiles with the Image Dissector Scanner attached to the Boller and Chivens spectrograph of the 3.6 m telescope. These are depicted for the same object in Fig. 5. The expected $P\alpha/H\beta$ ratio from unmodified recombination theory is 0.35 (where a temperature of 10,000 K and opaque conditions are assumed). In our two objects we find comparatively enhanced values: 1.24 ± 0.3 for the quasar and 0.73 ± 0.4 for the galaxy. They are also higher than those found by Puetter and Soifer 1981 who find a range for this ratio from 0.09 to 0.72 for their sources with the exception of PG 0026+129, for which Puetter et al. found the very high ratio of 1.4 in 1978 (R. C. Puetter et al., 1978, *Astrophys. J.*, Lett., **226**, L53). The deviation from the recombination value may be explained by reddening in the sources and/or by optical depth effects. However, we think that the high $P\alpha/H\beta$ ratios found by us indicate that the emission-line regions in nuclei are still poorly understood and substantial improvements in the line transfer calculations with and without dust absorption are necessary. Attempts in this direction are presently being done among others by R. C. Canfield and R. C. Puetter and by Mme S. Collin-Souffrin and collaborators.

Our observational results reported here are the subject of a more detailed paper (W. Kollatschny and K. Fricke, 1981, *Astron. Astrophys.*, in press). We are presently continuing our hydrogen-line observations in the infrared and optical spectral ranges using the ESO equipment and in the UV with the IUE

ANNOUNCEMENT OF AN ESO WORKSHOP ON

The Most Massive Stars

ESO Munich, 23–25 November 1981

Among topics to be discussed in the workshop are the theory of evolution of massive stars, observations of luminous stars in the Galaxy and nearby systems, the effect of the presence of these stars on the structure and evolution of the interstellar matter in galaxies and their use as distance indicators.

The workshop will include both review papers and short contributions with ample time for discussion.

Contact address:

S. D'Odorico,
Workshop on Massive Stars,
ESO
Karl-Schwarzschild-Str. 2
D-8046 Garching bei München

satellite telescope in order to obtain complete sets of Lyman, Balmer and Paschen ratios for a sample of active galactic nuclei. We thus hope to provide useful constraints to improve the theoretical descriptions.

Acknowledgement

This work was in part made possible by a grant (Fr 325/12 and Fr 325/15-2) of the Deutsche Forschungsgemeinschaft.

UBV Photometry of Quasars

G. Adam, Observatoire de Lyon

I. The Disappointed Hopes

1. Hubble and the Birth of Observational Cosmology

Between the two world wars, a few people were, surprisingly, still concerned by extraterrestrial problems. One of them was Edwin Hubble, who discovered the so-called expansion of the universe, after proving the extragalactic nature of the great nearby spiral galaxies. Since then, astronomers have tried to understand the large-scale geometry of that newly opened universe. It is a long and still unsuccessful story. . .

How can we use the extragalactic objects to study that large-scale structure? There are two powerful methods:

(a) Counts of distant objects, up to some limiting magnitude. The dependence of the number of objects found on the radius sampled in the universe can in principle tell us if our universe is spherical and closed, or euclidean, or hyperbolic and open (a euclidean universe is just the kind of universe we like, with non-crossing parallels and circle area obeying the good old r -square law). In fact, the deceleration parameter q is the crucial one which defines the overall geometry.

(b) Plots of the recession velocity – or of the redshift z – of distant objects as a function of their measured luminosity. If we assume that the different objects have the same intrinsic luminosity, this is equivalent to a plot of the recession velocity versus the distance. Usually, one constructs a plot of $\log z$

versus the apparent magnitude. For large values of z , the curves are very q -dependent and should tell us what is the "observational value", the one which fits best the experimental curves.

In fact, that approach initially failed: the most distant galaxies which can be observed are still too near to us, with z around 0.5. This is far too short an interval to allow a q determination.

2. Quasars: The Cosmological Boom

In the early sixties, a new class of extragalactic objects entered the astronomical scene: the quasi-stellar objects, or quasars. Now, we have at hand lists of such objects which should soon reach the 2,000 entries, with large redshifts up to 3.53, and a lot of photometric measurements, mainly UBV. So it seems that solving the cosmological problem is just a matter of drawing a large Hubble diagram, fit a curve to the observational points, and write q in golden letters in the Great Book of Astronomical Achievements. But Figure 1, which is a Hubble diagram tying the B magnitude to the redshift for 358 quasars, has a most unpleasant look. . . The accuracy of modern UBV photometry is too high to account for such a scatter. In fact, there are three main difficulties:

(a) Use of the Hubble diagram assumes that all the objects observed have the same intrinsic luminosity. Unfortunately, this is very far from truth for quasars: at the same redshift, the

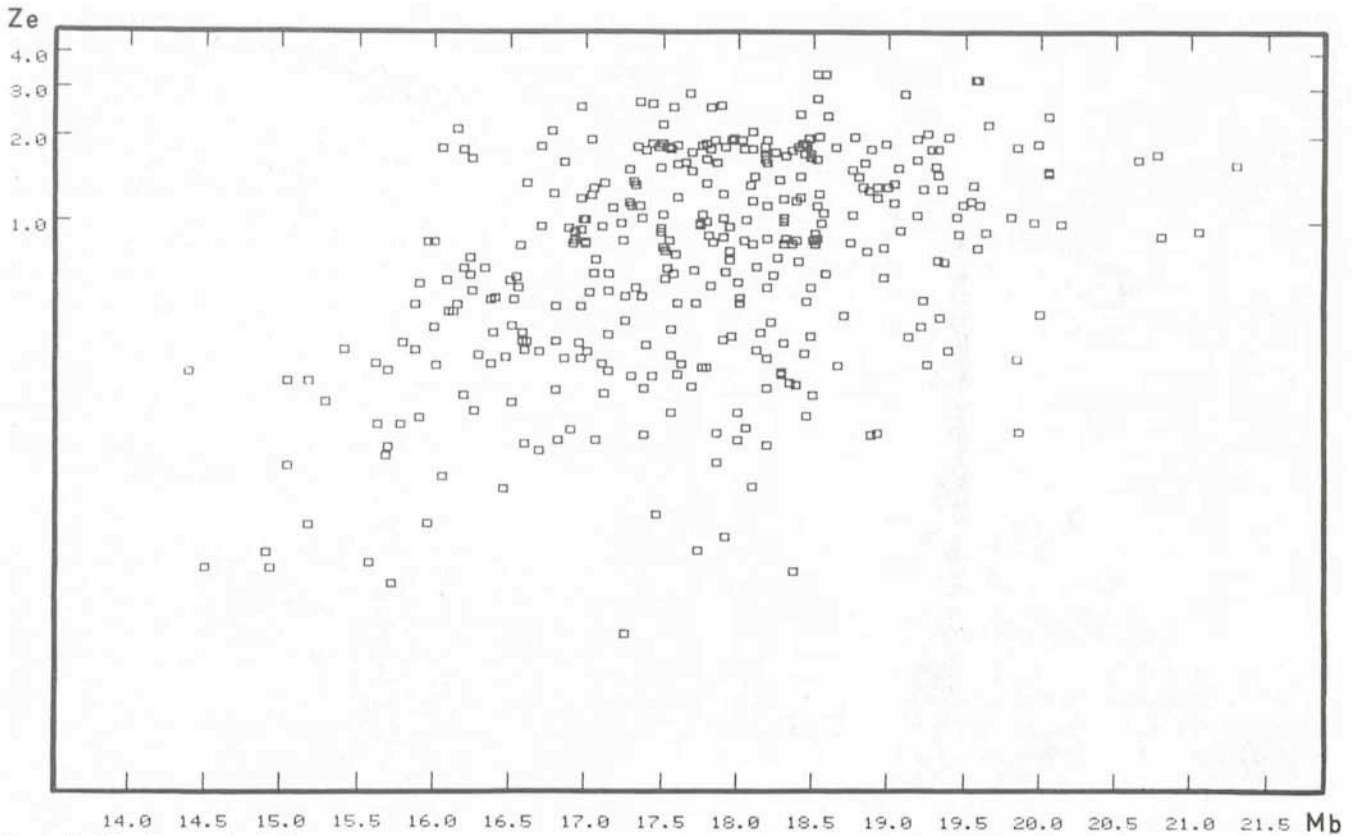


Fig. 1: Hubble diagram for 358 quasars.

magnitude of two objects can differ by several unities. More, a great number of objects are variable.

(b) At large redshifts, evolution effects become important, as we look at the objects as they were several billion years ago. And, up to now, we don't know which kind of evolution affects the quasars.

(c) The observational limits play very strongly in the high- z part of the Hubble diagram. We work at the very end of the photometric possibilities of our telescopes, and selection effects are enormous. For instance, is the cut-off at $z = 3.5$ real or due to some observational effects?

All this makes the Hubble diagram extremely difficult to work with. Great care must be taken in the statistical analysis.

II. Why UB V Photometry?

It seems that UB V photometry doesn't give very useful information: due to the redshift, the spectral features falling into the U, B and V bands can be anything, varying from one object to another. Photometry with fixed bands is, then, a very coarse tool to study those exotic and complicated quasars. So, why waste astronomers' time doing UB V quasar photometry?

Well, there are a lot of things that just can't be done in an easier way than with UB V photometry:

1. Optical Identification of Radio Sources

Radio sources are usually detected without any aid from optical astronomy. It is then important to seek for optical counterparts, radio galaxies or quasars. This is done by exploring the vicinity of the radio source position on a deep sky photograph. When one finds a stellar object, it may be a star (and it is a misidentification) or a quasar. The ultimate proof will be a spectrum of the object. That is a long and costly operation, when the object is faint, which is the usual case.

It has been known, for a long time now, that quasar colours (the indexes U-B and B-V for instance) are different from the colours of ordinary stars. Figure 2 shows a plot of B-V versus U-B for the quasars. The observational points are represented as "bubbles", the diameters of which grow as z . In the early times of quasar studies, Allan Sandage found a fairly good correlation between the position of the representative point of a

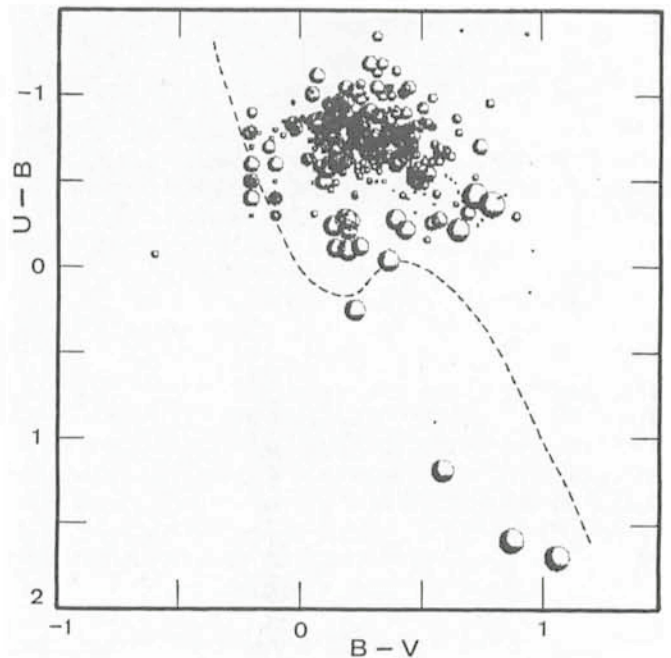


Fig. 2: Plot of U-B versus B-V for 384 quasars. The interrupted line is the Main Sequence for Galactic stars. Bubbles sizes vary as the redshift z .

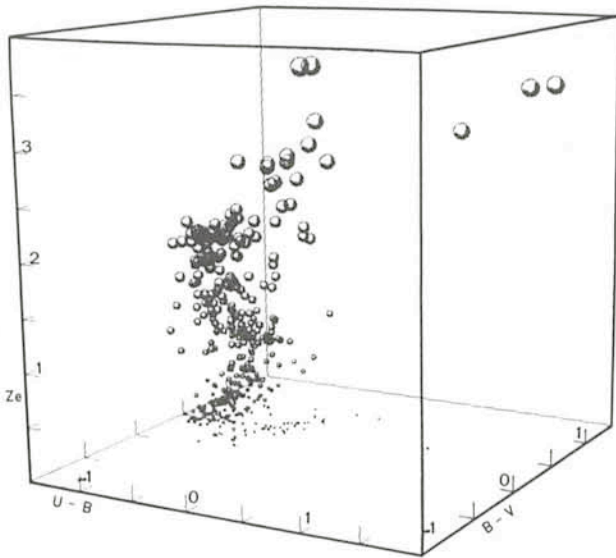


Fig. 3: Three-dimensional plot of U-B, B-V, and the emission redshift z_e . Bubbles sizes vary as z_e .

quasar and its redshift. This gave some hopes that the redshift determination may be replaced by a photometric UBV measurement, a much faster operation. But Figure 2 shows that, as the z-range increased, the correlation disappeared. The early

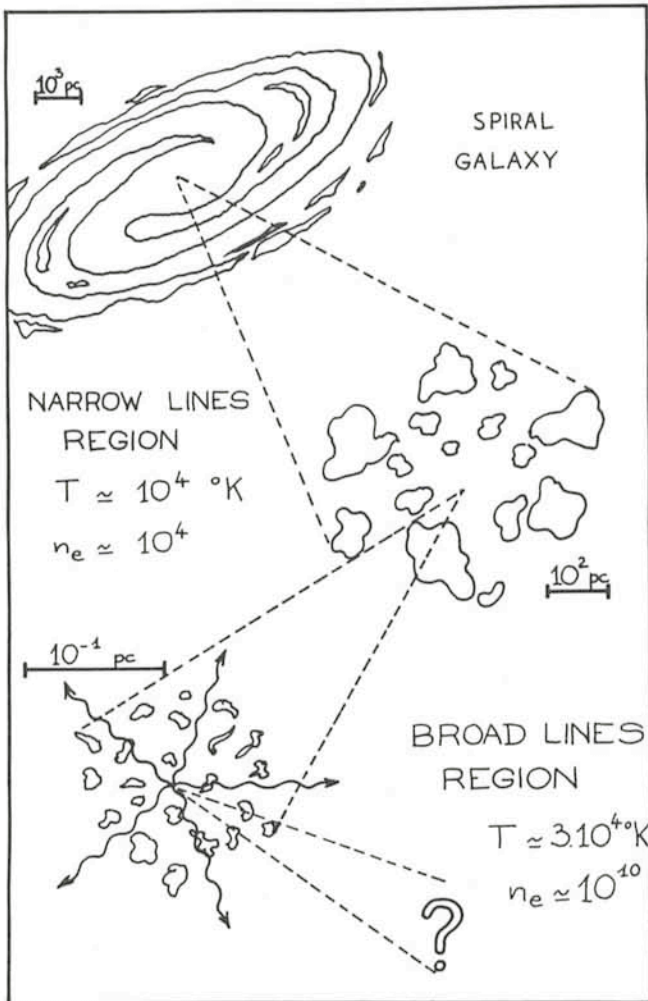


Fig. 4: Schematic view of a spiral galaxy with an active nucleus: one of these so-called quasars.

diagram of Sandage corresponds to the central over-crowded part of the present one. The very high redshift quasars are much "redder" and their representative points fall on the interrupted line where the bulk of the stars of the Galaxy are located. Figure 3, which is a three-dimensional plot including z as the third coordinate, shows that the U-B/B-V diagram is in fact the plane projection of a spiral path, and cannot be used alone.

Anyway, a quick UBV measurement of a quasar candidate can tell us, at the 90% confidence level, if it is or not a quasar. The usual criterion is something like U-B lower than -0.35 . Extremely few stars are so blue. So, it's good practice to use a middle-sized telescope for UBV photometry before spending one hour on each object doing spectroscopy with a large instrument. The couple 1 m/3.6 m on La Silla is an excellent example of such an association.

2. Hubble Diagram of Quasars

Since the first attempts made to use that diagram, the situation has deeply evolved. The sample of quasars with known B or V magnitudes has enormously increased: more than 1,700 today (but with widely varying accuracies). Several hundreds were measured with the ESO 1 m photometric telescope. More, the multifrequency data are growing fast, in radio, infrared, ultraviolet, X-rays or gamma-rays. So, it is now possible to grapple with the problem in a new way: first, quasars are classified according to some observational characteristics (non-radio or radio, flat or steep spectrum, and so on...). Then, with those more homogeneous classes, one can try a new study of the sub-Hubble diagrams. This is part of the work in progress in Lyon. As it may be supposed that different classes of quasars correspond to different evolutive stories, these differences should show up in the sub-Hubble diagrams.

3. Quasar Physics

Figure 4 gives a very simplified view of a typical (as far as that exists) active nucleus of galaxy, such as a quasar. From centre to outside, one finds:

(a) The central "motor", not yet completely understood, but which could be an accreting giant black hole, that is a black hole swallowing pieces of stars torn apart by tidal forces, according to some promising models. This central motor produces an enormous amount of non-thermal radiation which is responsible for the energy transfer between the black hole system and the outer world.

(b) A region partially filled with filaments and clumps of hot (around 30,000 degrees) gas, with high velocities (between, say 1,000 and 10,000 km/s). The clouds are partially or totally ionized by the central continuum, and emit the very broad emission lines which dominate the classical quasar spectrum. This region has a diameter of the order of one parsec.

(c) Farther away (a few hundreds of parsecs), float large clouds of relatively cold (10,000 degrees) and diluted gas, less turbulent, which are responsible for the narrow lines seen in quasar spectra.

How can UBV photometry help in the study of quasar physics? For instance, in two ways:

- It provides a quick manner of looking at the continuum emission. Figure 5 shows how the U-B index of quasars changes as the various emission lines are shifted across the photometric bands. For instance, one can see the change in colour around $z = 2.5$, where the very strong Lyman alpha emission line leaves the U band and enters the B band. So quasars with z greater than 2.5 look "redder". After making a UBV measurement, one can correct for the emission-line

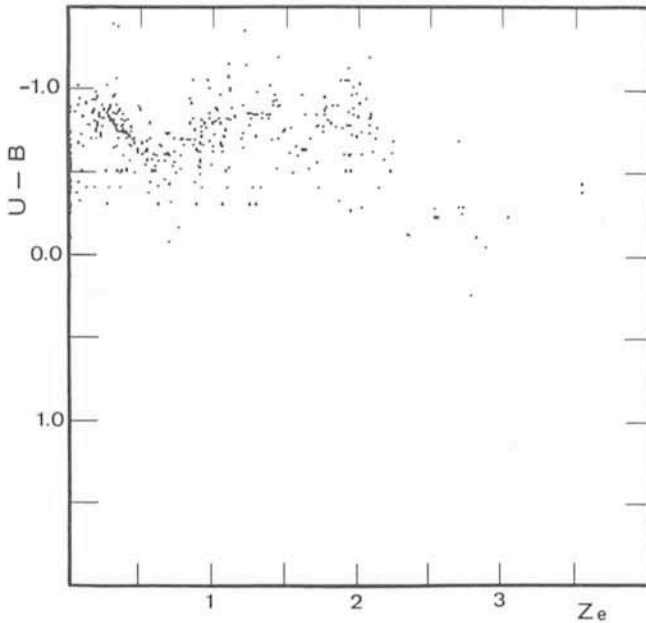


Fig. 5: Plot of $U-B$ versus Z_e for 384 quasars.

influence by using a standard emission-line quasar spectrum, and get a good approximation of the slope of the continuum. Less accurate than spectrophotometry, of course, but far quicker. As quasars have usually the bad taste of being very

weak objects, a wide band photometry is essential to grasp a maximum of those scarce photons.

– The central regions of the nucleus emit, often, a variable amount of energy. The monitoring of that variability is the only way to get information about the sizes of the emitting regions. A simple argument shows that if an object is variable on a time scale of, say, a week, its overall dimensions cannot be much in excess of one light-week. Otherwise, variations concerning different parts of the object would be “averaged” and such a short time scale would not be observed. We are now reaching the day level, and that is, more or less, the lower limit the present models can accept. Discovery of faster variations in quasars would call for a new improvement of those models. So it is extremely important to seek for such fast variations, and to include such observations in a multifrequency programme. As radio, visible and X-ray radiations originate in different regions, multifrequency monitoring should throw new light on the structure of active galactic nuclei of galaxies.

The technical difficulties are great, of course: searching for fast variations, one searches for faint variations. Once again, broad band photometry is the good choice, with a large telescope and as many nearby standard stars as possible, to minimize the unavoidable noise.

What else? Well, we are, regarding the quasar problem, in the data-accumulation phase. Nobody can tell exactly what is a quasar, and it is still necessary to accumulate a maximum of information, and to seek for a maximum of correlations between parameters. It’s the time where people plot anything versus anything, and hope to find some New and Universal Truth. . . . Magnitudes are just one of such parameters.

An Infrared Speckle Interferometer

C. Perrier, ESO

Since visible speckle interferometry has been developed ten years ago, efforts have been made to extend this technique to the infrared range for angular size measurements. Using the experience obtained on Kitt Peak by Sibille, Chelli and Lena (1979, *Astronomy and Astrophysics*, **79**, 315), an IR speckle interferometer has been developed at the La Silla observatory in connection with the installation of the IR photometer designed for the 3.6 m Cassegrain focus.

The aim of this article is to describe this system and to present the peculiarities of this observational technique in the light of selected results. But first let us recall the astrophysical motivation for such a work.

The Need for High Resolution at IR Wavelengths

The main motivation is the lack of direct information on the spatial intensity distribution in existing models of the various objects belonging to the group of compact IR sources. Among them, those found in regions of active star formation are probably the most fascinating.

As all their flux is emitted in the infrared, ranging from a few microns up to hundreds of microns, these objects are not reachable with optical interferometry. On the other hand, their size may lie within the diffraction-limited resolution of the large telescopes: Fig. 1 shows the radius of a $10 M_{\odot}$ protostar for three representative evolutionary times (taken from Yorke, 1980, *Astron. Astrophys.*, **85**, 215), assuming a diffraction-based limitation i.e. 0.12 arcsec at K (3.5 μm) and 0.27 arcsec at M (4.8 μm), we can see that this object, as far as 0.5 kpc, could be resolved at these wavelengths with a 3.6 m telescope.

Of course, other types of IR objects deserve an investigation at high resolution: IR/OH sources, giants or late-type stars with extended envelopes. For some Miras, size measurements at precise wavelengths corresponding to absorption features may reveal dynamical structures.

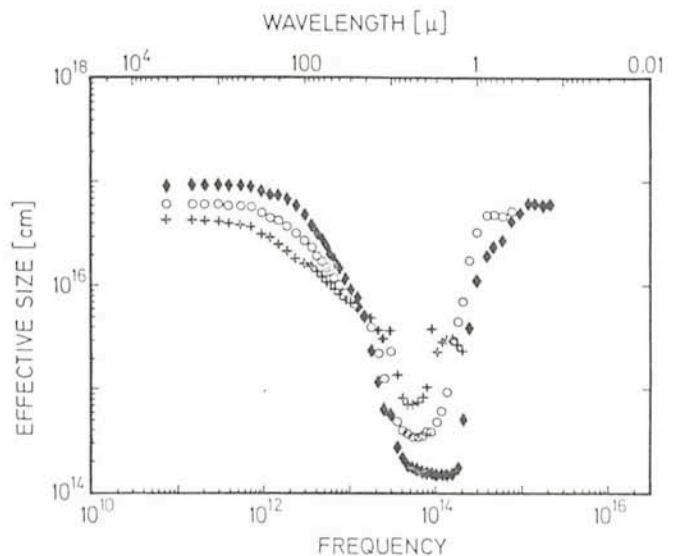


Fig. 1: Radius as a function of wavelength for a $10 M_{\odot}$ protostellar object model at three evolutionary times. At K (2.2 μ) and M (4.8 μ) size is ranging from 1.3 to $6.7 \cdot 10^4$ pc (from Yorke, 1980).